2021 ERDKUNDE Vol. 75 · No. 2 · 87–104

CLIMATE AND ENVIRONMENTAL CONTEXT OF THE MONGOL INVASION OF SYRIA AND DEFEAT AT ‘AYN JĀLŪT (1258–1260 CE)

Nicola Di Cosmo, Sebastian Wagner and Ulf Büntgen

With 7 figures, 1 table and 1 supplement
Received 13 April 2021 · Accepted 18 May 2021

Summary: After a successful conquest of large parts of Syria in 1258 and 1259 CE, the Mongol army lost the battle of ᶜAyn Jālūt against Mamluks on September 3, 1260 CE. Recognized as a turning point in world history, their sudden defeat triggered the reconfiguration of strategic alliances and geopolitical power not only in the Middle East, but also across much of Eurasia. Despite decades of research, scholars have not yet reached consensus over the causes of the Mongol reverse. Here, we revisit previous arguments in light of climate and environmental changes in the aftermath of one the largest volcanic forcings in the past 2500 years, the Samalas eruption ~1257 CE. Regional tree ring-based climate reconstructions and state-of-the-art Earth System Model simulations reveal cooler and wetter conditions from spring 1258 to autumn 1259 CE for the eastern Mediterranean/Arabian region. We therefore hypothesize that the post-Samalas climate anomaly and associated environmental variability affected an estimated 120,000 Mongol soldiers and up to half a million of their horses during the conquest. More specifically, we argue that colder and wetter climates in 1258 and 1259 CE, while complicating and slowing the campaign in certain areas, such as the mountainous regions in the Caucasus and Anatolia, also facilitated the assault on Syria between January and March 1260. A return to warmer and dryer conditions in the summer of 1260 CE, however, likely reduced the regional carrying capacity and may therefore have forced a mass withdrawal of the Mongols from the region that contributed to the Mamluks' victory. In pointing to a distinct environmental dependency of the Mongols, we offer a new explanation of their defeat at ᶜAyn Jālūt, which effectively halted the further expansion of the largest ever land-based empire.

Zusammenfassung: Am 3. September des Jahres 1260 n. Chr. unterlagen die berittenen Mongolen erstmals in ihrer überaus erfolgreichen territorialen Westexpansion gegen die von Süden aufmarschierenden Mamluken in der Schlacht von ᶜAyn Jālūt. Diese Niederlage im heutigen Israel markiert einen welthistorischen Wendepunkt, in Folge dessen das Machtgefüge nicht nur im Mittleren Osten, sondern über ganz Eurasien neukonfiguriert wurde. Gleichwohl der geopolitischen Relevanz und trotz zahlreicher Erklärungsversuche ist es Wissenschaftlern bis heute nicht gelungen, die Niederlage der Mongolen bei cAyn Jālūt überzeugend zu erklären. In der vorliegenden Studie berücksichtigen wir raumzeitlich hochaufgelöste Klima- und Umweltveränderungen nach dem Ausbruch des indonesischen Vulkans Samalas circa 1257 n. Chr. Sowohl die jahrringbasierten Rekonstruktionen, als auch die Klimamodelle deuten auf eine starke Abkühlung und generell feuchtere Bedingungen von 1258 bis 1259 hin. Die durch einen der wohl größten Vulkanausbrüche der letzten 2500 Jahre ausgelösten Klimaschwankungen müssen als wichtiger Faktor für die Verzögerung des Mongolenfeldzuges mit seinen geschätzten 120,000 Kriegern und bis zu einer halben Million Pferden angesehen werden. Kühlere und feuchtere Bedingungen haben demnach die Eroberung weiter Teile Syriens zwischen Frühjahr 1258 und Herbst 1259 begünstigt, wohingegen die Rückkehr zu einem wärmeren und trockeneren Klima im Sommer 1260 n. Chr. die Mongolen schwächte und somit wohl zu ihrer Niederlage bei ᶜAyn Jālūt beitrug. Unsere Studie verdeutlicht die starke Abhängigkeit der mongolischen Kavallerie von Umweltfaktoren und liefert einen neuen Erklärungsansatz für ihr Scheitern in Syrien, was letztlich eine weitere Expansion der größten Landmacht verhinderte.

Keywords: climate shocks, Eurasian steppe empires, human-environment interaction, model simulations, Mongol empire, proxy reconstructions, Samalas eruption, volcanic forcing

1 Introduction

The history of Eurasian steppe empires has been the object of several recent studies that have raised new questions and advanced new hypotheses regarding the complex interaction between human and natural factors (Büntgen et al. 2011, 2016; Oppenheimer et al. 2017), and the degree to which the latter impacted the rise, development, and demise of nomadic political formations (Di Cosmo et al. 2017, 2018; Ganiev and Kukarskih 2019). However, given that climatic variations are usually examined in their long-term effects rather than short-term shocks, it is exceedingly difficult to establish the precise connection between climate anomalies and their more or less immediate – direct

https://doi.org/10.3112/erdkunde.2021.02.02 ISSN 0014-0015 (Print) · ISSN 2702-5985 (Online)

and indirect – impact on historical events. Most critical in this regard is the availability of precisely dated natural and human archives (Büntgen and Oppenheimer 2020), such as tree ring-based climate reconstructions and written historical sources.

The Mongol empire (1206–1368 CE; all calendar dates hereafter are Common Era) has a unique place in world history as the largest continuous empire ever created and most powerful force ruled by pastoral nomads. Recent scholarship has focused on past climate variability in relation to the Mongols' reliance on the resources of the pastoral economy and their dependency on grassland productivity. In their military campaigns the Mongols relied on thousands of small but resilient horses (on average five per soldier), which needed to be fed and watered on local pastures wherever the army went. Seasonality played a central role in the planning of campaigns, based on the animals' life cycle and the availability of pasture. In their movements, the Mongols also exploited different altitudinal zones to compensate for climate variations that were either too warm or too cold, and may thus compromised the health of both people and horses. The Mongol campaigns and their objectives were therefore closely dependent upon the carrying capacity of the land and other biogeographic factors, such as topography, vegetation and water supply. Previous studies successfully assessed the environmental impact of climate variability on the history of the Mongol empire (Pedersen et al. 2014; Büntgen and Di Cosmo 2016; Putnam et al. 2016).

Here, we present a new interpretation of the Mongol campaign in Syria between 1258 and 1260 in the light of climate and environmental variability in the aftermath of the Samalas volcanic eruption circa 1257 (Fig. 1). Based on high-resolution ice core evidence of bi-polar sulfate accumulations (Sigl et al. 2015), the Samalas eruption was most likely the largest volcanic event in the past 2,500 years, which possibly caused distinct regional- to large-scale summer cooling and precipitation surplus in the first years after the eruption (Wade et al. 2020; Guillet et al. 2017; Stoffel et al. 2015; Büntgen et al. 2017, Piermattei et al. 2020). The examination of the Mongols' advance into Iran, Iraq, Syria and Palestine shows that climate and environmental factors may have played an important role in critical choices made by Hülegü, the Mongol chief commander, and his generals in the timing and deployment of military resources. While the direct impact of environmental factors remains hypothetical, the combined paleoclimatic and historical evidence now suggests, for the first time, that both the Mongol invasion of Syria and the subsequent withdrawal of the bulk of their army were affected by extraordinary climate conditions after one of the largest volcanic eruptions of the past 2,500 years.

2 Materials and methods

2.1 Proxy reconstructions, model simulations and re-analysis data

Since our study at the interface of past climate variability and human history requires annual dating precision (Büntgen and Oppenheimer 2020), we restricted our proxy evidence to tree-ring records that provide the necessary temporal resolution. Although not directly representing the area of interest, for which no such records cover the mid-13th century, we used three regional tree ring-based summer temperature reconstructions from the Spanish central Pyrenees (Büntgen et al. 2017), the Swiss Alps (Büntgen et al. 2006), and the Russian Altai (Büntgen et al. 2016), as well as a most recent dendro-based Eurasian-wide summer temperature reconstruction (Büntgen et al. 2020). Furthermore, we used five tree ring-based reconstructions of warm-season hydroclimate variability from Morocco (Esper et al. 2007), Greece (Cook et al. 2015; Klippel et al. 2018; Esper et al. 2021), and Turkey (Griggs et al. 2007). Information from the individual temperature and hydroclimate reconstructions is restricted to the corresponding growing season, which is best averaged over the June–August period. While all reconstructions are expected to be most accurate on interannual to decadal time-scales, some of the hydroclimatic records might be limited in preserving low-frequency variations. However, this possible constraint is not important for our study, which focuses on the year-to-year variability between 1256 and 1260. It should be further noted that the summer temperature reconstructions generally explain more variance over relatively larger spatial domains, whereas the hydroclimatic reconstructions are associated with wider uncertainty ranges and overall smaller areal validity, which is associated with a lower spatial de-correlation distance and co-variability (Büntgen et al. 2010).

In order to validate our regional proxy evidence and provide additional paleoclimatic insights with seasonal resolution, we used the comprehensive Earth System Model (ESM) simulations from the PMIP3 repository on the Earth System Grid Federation (https://esgf-data.dkrz.de/projects/esgf-dkrz/). We restrict ourselves to the analyses of two ESMs related to CCSM4 and MPI-ESM-P forced with the PMIP3 protocol. The CCSM4 model (Landrum et al. 2013) consists of the Community Atmospheric Model 4 (CAM4). The original horizontal resolution is 1.258° latitude x 0.98° longitude with 26 vertical layers. The ocean model is the Parallel Ocean Model version2, with a 1° horizontal resolution, increasing in latitude from 0.54° at 33° North towards 0.27° at the equator. The ocean model has 60 vertical levels. The land model refers to the Community Land Model 4 (CLM4), including submodules for hydrology, land use and carbon–nitrogen biogeochemistry. For this configuration, only one realization implementing the volcanic forcing by Gao et al. (2008) is available. Solar activity changes are based on Vieira et al. (2011), and the land-use changes are taken from Pongratz et al. (2008). The MPI-ESM-P-LR model (Giorgetta et al. 2013) consists of the atmospheric component ECHAM6 and the ocean component MPI-OM. The horizontal resolution of ECHAM6 is T63 (approx.1.9° horizontal resolution) with 47 vertical levels. The MPI-OM is integrated on a curvilinear bipolar grid (~1.5° resolution near the equator) with 40 vertical levels. The land model is JSBACH, allowing for an interactive simulation of vegetation and land cover changes. For the simulations under investigation, pre-scribed vegetation maps from Pongratz et al. (2008) are used. For the MPI-ESM-LR, three ensembles are analyzed (Jungclaus et al. 2014), with realizations 2 and 3 not being official part of the CMIP5/PMIP3 repository. The differences in the realizations relate to differences in initial conditions in the year 850 when the model simulations start. All simulations are forced with the same protocol of the first realization. Specifically, changes in volcanic activity are based on the Crowley and Untermann (2013) dataset. Changes in solar activity are also based on the reconstruction of Vieria et al. (2011).

The data we use for producing climatology fields for present-day climate over the eastern Mediterranean and Arabian region are based on the ERA40 reanalysis project (Uppala et al. 2005). The advantage of this dataset is that, in addition to meteorological station information, it uses assimilation of satellite imagery produced by the European Centre for Medium-Range Weather Forecasts (ECMWF). This is especially important for investigations over regions with a sparse observational network. We downloaded monthly mean values for near-surface temperature and total precipitation, with the latter consisting of convective and stratiform contributions. We chose the 1959–1990 period as a climatological reference period for both the summer (April–September) and the winter (October–March) half year. The rationale in presenting the present-day climatology is to underpin the strong regional and seasonal deviations of near-surface temperature means and precipitation totals caused by the Samalas eruption ~1257, and to provide a comparison for the paleo-model simulations.

2.2 Historical documentary evidence

The Mongol invasion of Syria has been documented in a variety of sources (Fig. 2), predominantly Arabic and Persian ones. In the present study we have consulted relevant passages from the following works, which have been examined largely through established translations and secondary works. A major source is the *Compendium of Chronicles* (*Jami'ut Tawarikh/Jami' al-Tawarikh*) by the Ilkhanid court historian Rashid Ad-Din (1247–1318), of which we have both Persian and Arabic manuscripts (thackston 2012). Another essential Persian source is the work by Ata-Malik Juvaini (1226–1283), a contemporary of the Mongol conquest who was with Hülegü during the expedition, and wrote the *Tārīkh-i Jahāngushāy* (History of the World Conqueror) detailing the Mongol conquest (Boyle 1958). An Arabic source is the history of Egypt by the Mamluk historian Al-Makrizi, which is his history of Ayyubid and Mamluk rulers, translated by Etienne Quatrèmere (Makrizi 1845). The Syriac *Chronography* by Gregory Bar Hebraeus (1226–1286) also provided some valuable information (Hebraeus 1932). The work by the Armenian historian Kirakos Ganjakets'i was also consulted (Bedrosian 1986). A Latin source that is central to this article is a letter sent by Hülegü, whose text has survived (Meyvaert 1980). Other works consulted but not cited because no sufficient evidence was found were the Persian chronicle by the Illkhanid historian Waṣṣāf (*fl.* 1265–1328), *Tārīkh-i Waṣṣāf*), or the *Gestes des Chiprois* (in old French*)* as well as other works such as the geographical and historical sources by the Armenian Hayton of Korykos, known as *La Flor des Estoires d'Orient* (*Flos Historiarum Terre Orientis*).

Fig. 1: The Mongol campaign in Iran, Iraq and Syria in the mid-13th century. (A) Geographical characteristics of the preparation, departure and travel of the Mongols from Karakorum to Bistām between 1252 and 1256. The green star indicates the location of ᶜAyn Jālūt. The red circles refer to the location of three regional tree ring-based summer temperature reconstructions in the Pyrenees, Alps and Altai. The dashed frame indicates the spatial domain of a tree ring-based Eurasian summer temperature reconstruction, and the blue circles refer to the location of five regional tree ring-based warm-season hydroclimate reconstructions from Morocco, Greece and Turkey. (B) A more detailed view on the Mongol campaign in the Middle East between fall 1256 and September 1260. Numbers in the maps refer to sites of the Mongol campaign. For details, refer to Tab. 1. Base map source: https://www.naturalearthdata.com.

3 Results and discussion

3.1 Reconstructed and simulated climate changes and environmental responses

Three regional tree ring-based summer temperature reconstructions from the Spanish central Pyrenees (Büntgen et al. 2017), the Swiss Alps (Büntgen et al. 2006), and the Russian Altai (Büntgen et al. 2016), as well as the most recent dendro-based Eurasian-wide summer temperature reconstruction (Büntgen et al. 2020) indicate a sharp temperature depression in the growing season of 1258 (Fig. 3A). While the reconstructed warm-season temperatures in the Pyrenees and Alps are almost back to normal in 1259 and 1260,

Tab. 1: Synthesis of chronological and geographical information of the Mongol campaign in the Middle East in the 1250s (see Fig. 1A-B for further information).

Fig. 1	Date	Event	Location	Region
1	1252 to 1254	preparation	inner Eurasia	Mongolia
2	fall 1254	departure	Karakorum	Mongolia
3	1254 to 1255	travel	Zaysan	Kazakhstan
4	1254 to 1255	travel	Ayagoz	Kazakhstan
5	1254 to 1255	travel	Almaty	Kazakhstan
6	summer 1255	travel	Almalyk	Uzbekistan
7	fall 1255	travel	Samarkand	Uzbekistan
8	1 Jan 1256	river crossing	Amu Darya	Uzbekistan
9	late winter 1256	travel	Sheberghan	Afghanistan
10	spring 1256	travel	Tun	eastern Iran
11	summer 1256	travel	Tus	eastern Iran
12	2 Sep 1256	arrival	Bistām	north-central Iran
13	fall 1256	campaign	Bistām	north-central Iran
14	7 Nov 1256	attack	Alamut	western Iran
15	winter 1256 to 1257	basecamp	Qazvin	western Iran
16	26 Apr 1257	arrival	Dinavar	north-west Iran
17	spring 1257	basecamp	Mughan	north-west Iran
18	Sep 1257	travel	Tabriz	western Iran
19	Sep 1257	travel	Hamadan	western Iran
20	19 No 1257	departure	Hamadan	western Iran
21	22 Jan 1258	arrival	Baghdad	northern Iraq
22	Mar 1258	departure	Baghdad	northern Iraq
23	Mar 1258	travel	Tabriz	western Iran
24	fall 1258	attack	Mayyafariqin	eastern Turkey
25	winter 1258 to 1259	pause	Mayyafariqin	eastern Turkey
26	summer 1259	revolt	Caucasus	Georgia
27	Sep 1259	departure	Mughan	north-western Iran
28	fall 1259	campaign	Jaziīa	eastern Syria
29	fall 1260	reinforcement	Mayyafariqin	eastern Turkey
30	Dec 1259	river crossing	Euphrates	northern Syria
31	15 Jan 1260	siege	Aleppo	western Syria
32	Feb 1260	surrender	Damascus	southern Syria
33	Mar 1260	siege	Mayyafariqin	eastern Turkey
34	7 Jun 1260	travel	Akhlat	eastern Turkey
35	summer 1260	arrival	Azerbaijian	north-western Iran
36	summer 1260	attack	Sidon	Lebanon
star	3 Sep 1260	battle	ᶜAyn Jālūt	Israel

Fig. 2: Mongols besieging Baghdad in 1258. Source: Jāmiʿ al-tawārikh [Compendium of Chronichles] by Rašīd al-Dīn Fazlullāh Hamadānī, c.1430-1434 [1307]. Bibliothèque nationale de France. Département des Manuscrits. Supplément Persan 1113, fol. 180v-181. Public domain: https://commons.wikimedia.org/wiki/File:Bagdad1258.jpg

the corresponding estimates from the Altai and the Eurasian-wide network reveal a slightly longer summer cooling until at least 1259. Five independent tree ring-based estimates of warm-season hydroclimate from Morocco (Esper et al. 2007), Greece (Cook et al. 2015; Klippel et al. 2018; Esper et al. 2021), and Turkey (Griggs et al. 2007) reveal overall wetter growing season conditions from 1259–61 (Fig. 3B). Interestingly, two records from Greece suggest relatively dry summer conditions in 1258. While the reconstructed, regional to larger-scale summer cooling in 1258 is remarkable in the context of 13th-century temperature variability (Fig. 4A), the tree ring-based evidence for wetter growing seasons in the aftermath of the Samalas eruption is not exceptional when compared to the range of natural hydroclimatic changes between 1200 and 1300 (Fig. 4B).

Given the limited quality and quantity of the available annually resolved and absolutely dated climate proxy data for the 13th century in the Middle East (Luterbacher et al. 2020) monthly resolved climate model simulations are needed for the period 1256–1260 to provide a more pronounced picture of the direct and indirect effects of climate and environmental change on the Mongol's conquest of Syria and defeat at ᶜAyn Jālūt. In line with historical and proxy evidence, one realization of the CCSM4 simulation exhibits exceptional cooling in the Middle East for the summer half year (April–September) of 1258–60 (Fig. 5). The coolest simulated half-year anomaly of up to 7 Kelvin occurs in the winter (October–March) of 1258–59 over much of Europe and the larger Mediterranean region. This is the period in which the Mongol army remained stationary in northern Iran, and difficulties were met in the siege of Mayyafariqin.

The simulation also shows wetter than average conditions from the fall of 1258 to the spring of 1260 over the Middle East. The simulated CCSM4 precipitation pattern is consistent with historical evidence of environmental changes, supporting the fact that the surplus in precipitation throughout the summer half year was favorable to support the large number of Mongol soldiers, horses and livestock in the aftermath of the Samalas eruption in the Middle East (Fig. 6). In addition, three ensemble simulations of the MPI-ESM-P model confirm the general temperature and precipitation response to the eruption (see Supplement II, Figs. S1–S6 for details). The precipitation patterns are less clear cut, especially within the three-member ensemble of the MPI simulations (Supplement II, Figs. S4–S6). This is in line with the overall limitations of Earth System Models to simulate precipitation patterns realistically in space and time. This caveat is most pronounced in those simulations that do not contain explicit data assimilation.

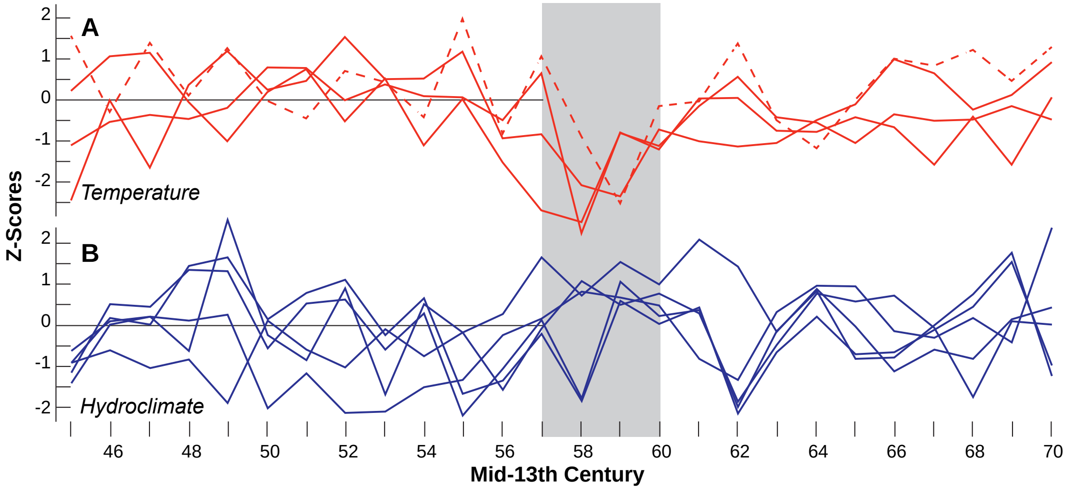

Figure S1. Simulated temperature anomalies from winter 1256–57 to summer 1260. Based on the MPI-ESM-P_r1 model, maps on the left and right sides refer to the six-month average winter (October–March) and summer (April–September) summer seasons, respectively. All values are in Kelvin, and expressed as anomalies to the pre-Samalas period 1225–1254.

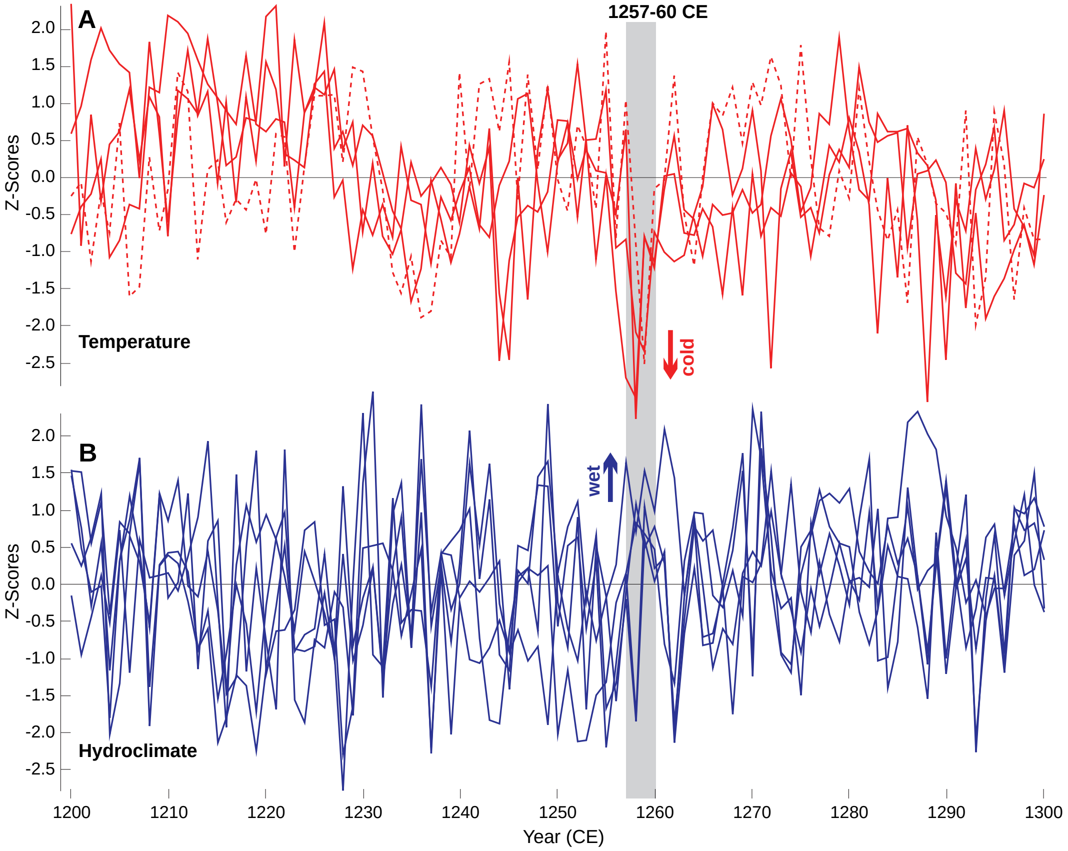

Fig. 4: Reconstructed climate variability of the 13th century. (A) The red lines are three regional tree ring-based summer temperature reconstructions from the Spanish central Pyrenees, the Swiss Alps, and the Russian Altai, whereas the dashed red line refers to Eurasian-wide summer temperature changes. (B) The blue lines are five regional tree ring-based hydroclimatic reconstructions from Morocco, Greece, and Turkey. The grey shading refers to the post-Samalas climate anomaly between 1257 and 1260.

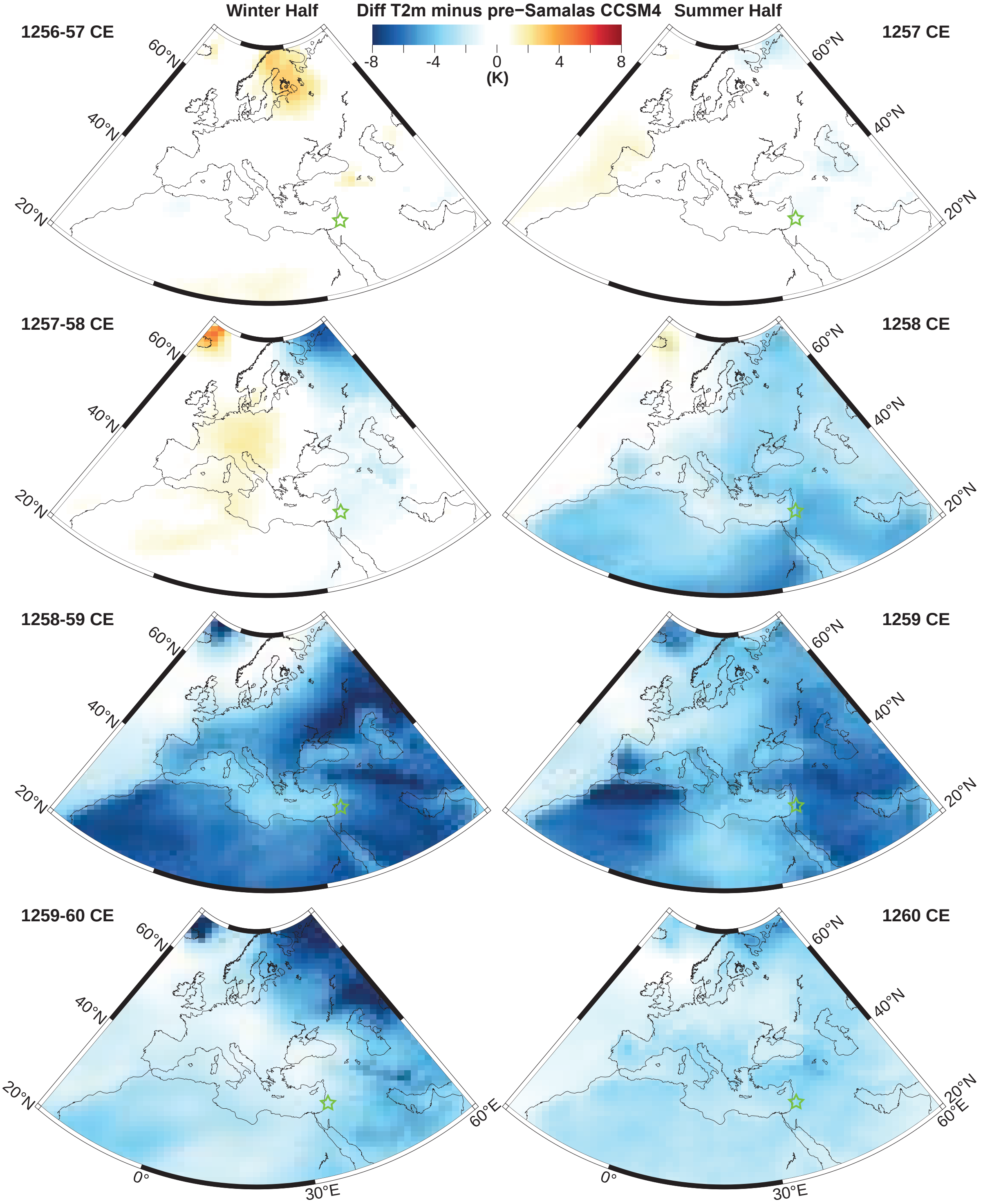

Fig. 5: Simulated temperature anomalies from winter 1256–57 to summer 1260. Based on the CCSM4 model, maps on the left and right sides refer to the six-month average winter (October–March) and summer (April–September) summer seasons, respectively. All values are in Kelvin, and expressed as anomalies to the pre-Samalas period 1225–1254 (see Supplement II, Figs. S1–S3 for comparable model output). The green star indicates the location of ᶜAyn Jālūt.

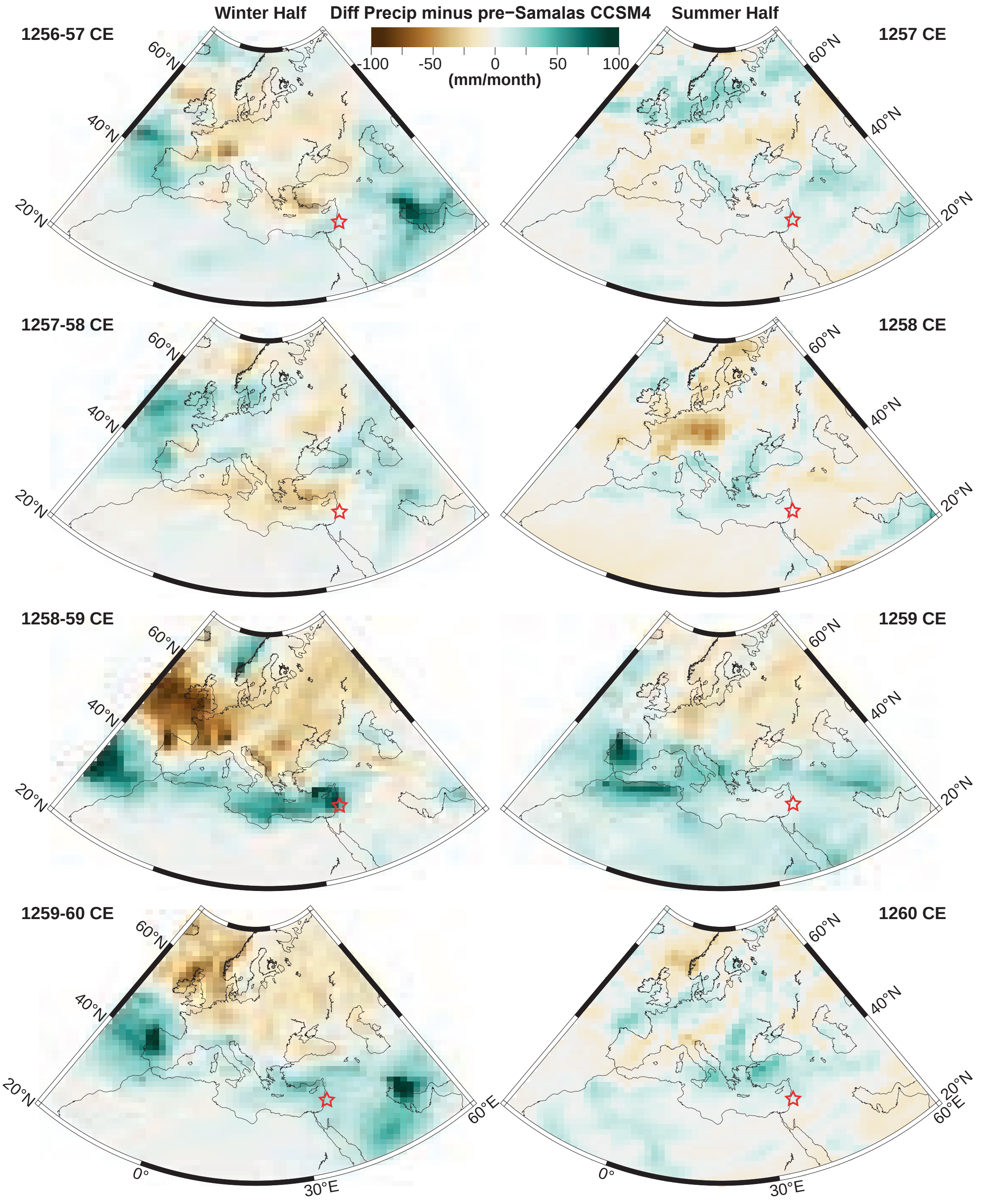

Fig. 6: Simulated precipitation anomalies from winter 1256–57 to summer 1260. Based on the CCSM4 model, maps on the left and right sides refer to the six-month average winter (October–March) and summer (April–September) seasons, respectively. All values are in millimeter per month, and expressed as anomalies to the pre-Samalas period 1225–1254 (see Supplement II, Figs. S4–S6 for comparable model output). The red star indicates the location of ʿAyn Jālūt.

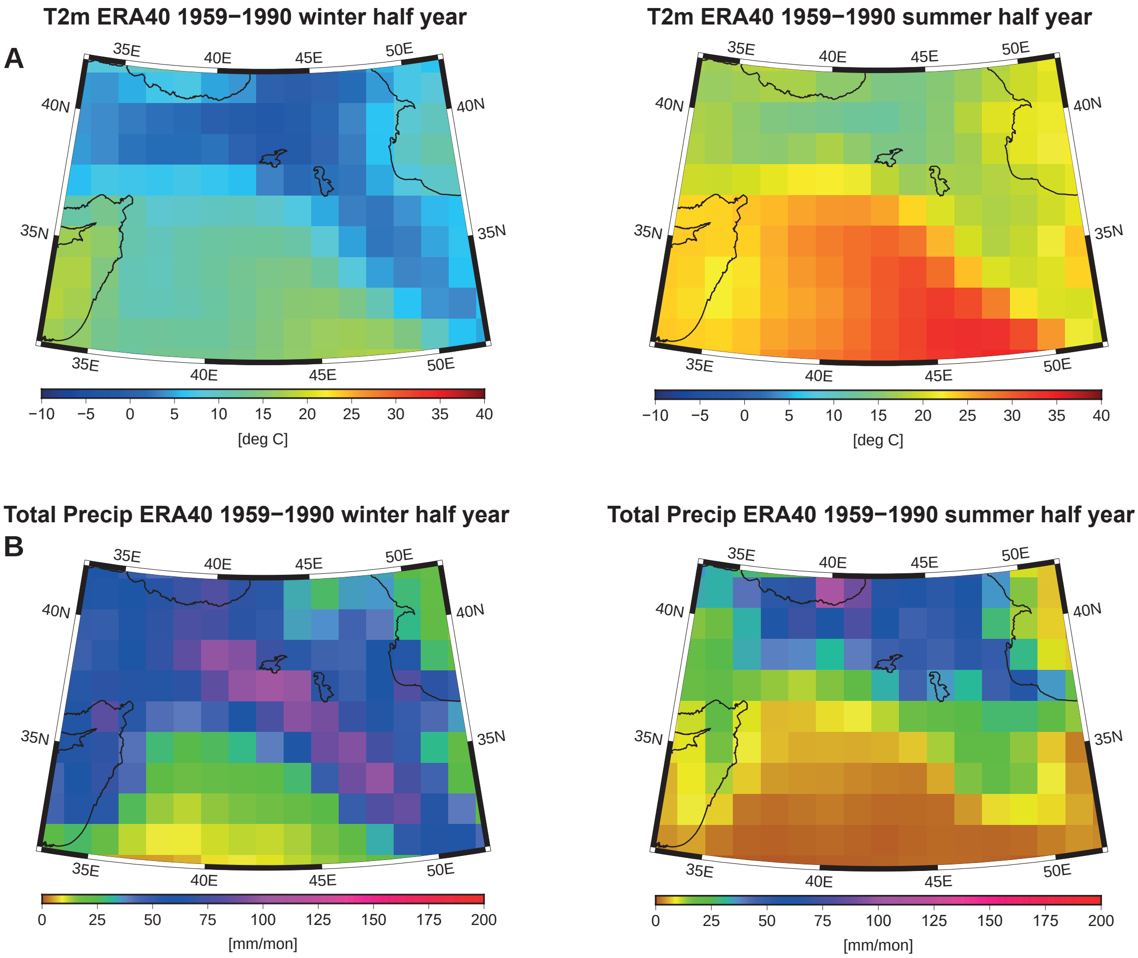
T2m ERA40 1959−1990 winter half year

T2m ERA40 1959−1990 summer half year

Total Precip ERA40 1959−1990 winter half year

Total Precip ERA40 1959−1990 summer half year

Fig. 7: Recent climatology. Mean climate conditions for near-surface temperature (left) and total precipitation (right) for the winter half (upper) and the summer half (lower) season for the ERA40 re-analysis data for the period 1960–1990. Note the very hot and dry summers over the region of Iraq and Syria during summer and the very low temperature during the winter season over the northern mountain chains. For the summer season, very dry conditions prevail in the present-day climate over the fertile crescent.

The overall differences in the simulated temperature amplitude likely result from different strengths of the volcanic forcing used (Crowley and Unterman 2013; Gao et al. 2008). For MPI-ESM-P simulations, volcanic reconstructions of Aerosol Optical Depth (AOD) based on Crowley and Unterman (2013) were used, whereas for CCSM4 the reconstruction of Gao et al. (2008) was implemented. The difference is approximately a 30% increased AOD values for Gao et al. (2008) compared to Crowley and Unterman (2013). This needs to be considered when comparing results from the different model simulations, especially concerning the magnitude of climatic changes in the aftermath of the Salamas eruption. However, consideration of the direct output from global climate models, even on an annual transient basis, is justified by the by the estimated magnitude of the Samalas eruption (Vidal et al. 2016). Eruptions of this size exert a pronounced impact on global climate and circulation patterns, which should be reflected coherently in different model simulations. Although a coherent picture of cooler and wetter conditions from approximately the summer of 1258 to the spring of 1260 is drawn for the greater Syrian region from independent lines of proxy and model evidence, caution is advised since the tree ring-based reconstructions are limited to the warm season and associated with large uncertainty ranges, and none of the ensemble model simulations can reproduce the exact evolution of the Earth's climate system due to the presence of internal climate variability.

To put the historical information into context, the present-day climate conditions represent an important factor to set the stage for environmental conditions, framing human activities, and influencing the strategy and fate of the Mongol army with profoundly changed conditions in the aftermath of the Samalas eruption in the middle of the 13th century. For the 2m-temperatures strong horizontal contrasts are evident over the focus region between the highlands of the Caucasus and northern region, and the low-lying region of Iraq and Syria (Fig. 7). This thermal contrast is pronounced during the winter half year, when the strong continental climate of the western interior of Eurasia is controlling the mean temperature pattern. For the summer, the general north-south contrasts are still evident, although their strength is strongly reduced because of high solar insolation with low cloud cover over the continental parts and the increase in the conversion from direct solar radiation into sensible heat. The precipitation pattern over the region of interest shows even stronger gradients between the regions north of Iraq and the Fertile Crescent extending into Syria. Year-round precipitation values are very low and are mostly due to winter half year precipitation. For this situation, it is important to notice the ecological consequences to support large troops with very little water supply, especially during the hot and dry summer season. Other salient territorial features in relation to the requirements of the Mongol army concern altitude and pasture.

Inferences regarding the impact of climate variability and overgrazing on semiarid regions are based on ecological research. First, numerous studies have shown that available moisture is the main driver of productivity in drylands (Le Houérou et al. 1988; Sullivan and Rhode 2002). This means that while rising temperatures and below-average precipitation reduce the overall production of grass, cooler temperatures reduce evapotranspiration, and more abundant precipitation increases above-ground biomass (Kgosikoma and Batisani 2014; Han et al. 2018). Intensive stockbreeding, leading to overgrazing, is held as a major cause for the depletion of the steppe rangelands in Algeria (Martínez-Valderrama et al. 2018), and current studies on the Syrian steppes (*Badia*) have likewise identified overgrazing as a major cause of land degradation (Louhaichi et al. 2012; Louhaichi and Tastad 2010). The negative impact of overgrazing in various climatic regimes has also been shown in the semiarid steppes of Inner Mongolia (Zhao et al. 2005; Qi et al. 2011), northern China (Wiesmeier et al. 2012; Han et al. 2018), as well as other grasslands (Garibaldi et al. 2007; Abdulahi et al. 2016), even though thresholds apply (Xie and Sha 2012). Based on these studies, it can be concluded that while the Syrian steppe gained from climatic cooling associated with the Samalas eruption in 1258–1259, intense grazing due to the sudden introduction of large numbers of herbivores in early 1260, coupled with a return to a regime of low rainfall and high levels of evapotranspiration, not only exhausted available pastoral lands, but required a substantial reduction of the livestock to allow them to recover. Such a recovery could not have been achieved without a withdrawal of the larger part of the military herds.

3.2 Climate and environmental context of the Mongol invasion of Syria and defeat at ᶜAyn Jālūt

The logistical complexity of the Mongol campaign in the Middle East (Fig. 1) can be appreciated from the two-year-long preparations that preceded Hülegü's departure from Mongolia in the fall of 1254 (Boyle 1958). No figure is given for the size of the Mongol army at the start of the campaign, except that it included one-fifth of the 'Eastern and Western armies' (Boyle 1958), which is difficult to estimate. However, the size of the Mongol army in the invasion of Khwarezmia in 1219, with a much smaller population base, was around 100,000 (Martin 1950). Moreover, considering the multi-year preparation, and an estimated size of the army that assaulted Baghdad in 1258 of about 150,000 (Smith 2006) - even though this included Mongol troops previously stationed in Iran and Anatolia - it is unlikely that Hülegü's army could have had less than some 120,000 warriors and about 600,000 horses (five per soldier).

The Mongol army proceeded slowly across Kazakhstan and into central Asia, reaching Samarkand in the fall of 1255, crossing the Amu Darya in January 1256 and then stopping in Afghanistan, where they met a frigid winter (Thackston 2012). The army resumed traveling in the spring of 1256, crossing into Iran and veering to the north, towards Khorasan (Tab. 1, 1-11). Tracing the progress of the Mongol army from its departure point to north-central Iran, we can see that it advanced across different biogeographic and climatic zones, which presented a wide range of challenges and imposed a careful choice of the route and resources to ensure that the horses could be fed and watered regularly and sufficiently (Potts 2014). Tactical planning, based on seasonality of movements and available pastureland, imposed flexibility to account for regional variations. In the last instance, the success or failure of the Mongols depended to a large extent on their careful balancing of the forces required to achieve their strategic objectives in relation to the available resources, which is to say, how many soldiers, horses, and livestock a given task would require and a given territory could support, and for how long. The speed of advance was relatively modest, on average about 15 miles per day, mostly due to long pauses between movements (Smith 2006). Changes in weather and topography clearly affected Mongol operations.

The route of the Mongol army into and across Iran in 1256-57 followed the pastures available along the alpine slopes of the Kopet-Dag mountain chain in Khorasan (Fig. 1A; Tab. 1, 11-12), located to the north of the deserts of central Iran. The army then wintered in areas rich in grassland, such as the Qazvin region (winter of 1256–57). The military operations against the Ismaili sect of the Assassins, in the mountainous area of Maymun Diz, began in early November 1256 and were timed to be completed before the onset of winter, although the Ismailis tried to slow the Mongols down, probably to take advantage of the cold weather (Thackston 2012) (Fig. 1B; Tab. 1, 13-16).

The main base of operations of the Mongol army was eventually established in the Mughan steppes (Tab. 1, 17), in today's Iranian Azerbaijan, a region that had previously been occupied by the forces of the main Mongol commander in the region, Baiju (Jackson 2017; Dashdondog 2010). Although this is a region that may have been able to accommodate several million animals, based on recent estimates (Alizadeh 2007), it is possible that the arrival of Hülegü's large army saturated the region's available pasture, since Baiju was forced to move his troops to a new base in Anatolia (Potts 2014; Dashdondog 2010). In the summer and fall of 1257 the Mongol army deployed between Tabriz and Hamadan. The grasslands in the Zagros Mountains as well as other pastoral areas may have supported the Mongol army in preparation of the campaign against Baghdad, which began in November 1257. This timing is especially significant because it coincides with peak condition of horses fed on summer pastures at higher elevations and with the fall of temperature in especially arid zones, such as Iraq (Tab. 1, 18-22).

After marching and arranging the various Mongol forces for two months, Hülegü ordered separate armies to converge on Baghdad in January 1258 (Fig. 2). The total Mongol force may have amounted to 150,000 soldiers, and presumably over half a million horses, including Armenian, Georgian, and local Muslim allies (Smith 2006). The region must have been able to sustain several hundred thousand horses for the duration of the operations, until March, when Hülegü and the largest part of the army withdrew to Iran along the same route through Hamadan and Tabriz, near which he established the capital of Maragha. As we can see, the seasonal pattern of Mongol operations was adjusted to the climatic characteristics of the place, preferring to fight in winter and withdrawing in the spring. The region around Baghdad, because of the extensive water system and fertile lands, was presumably able to support a large army without suffering too much from environmental depletion. The fall of Baghdad put an end to the Abbasid Caliphate, and the Caliph himself Al-Mustas'im was executed. The impact of the Mongol victory on the Islamic world was enormous. The Mongols remained in control of the region after various notables surrendered and thereafter the bulk of the army returned to Iran. During the winter, uncharacteristically, Hülegü's army remained stationary in Azerbaijan for over a year, from the summer of 1258 to the fall of 1259 (Tab. 1, 23).

Historical evidence points to worsening climatic conditions during the same period. Several sources mention famines and food shortages in 1259 and 1260 (Makrizi 1845, II: 81-82; Hebraeus 1932, 431, 436-437). Moreover, popular rebellions against excessive Mongol taxation in the kingdom of Georgia in 1259 are a significant indicator of extreme economic hardship (Lane 1999). Extensive famines and rebellions are indicative of food shortages due to crop failures possibly caused by colder and wetter climate that affected in particular mountainous areas in the Caucasus (Tab. 1, 26). Further evidence of possible climatic change is provided by one the few military failures. Around the end of 1258 a Mongol army was sent to take the stronghold of Mayyafariqin in Upper Mesopotamia (the Jazīra), which managed to hold out until the spring of 1260 (Amitai-Preiss 2011) (Fig. 1B and Tab. 1, 24-25, 29). The unusually long siege encountered enormous difficulties, and while stiff resistance is acknowledged, climate conditions appear to have played a significant role on both sides. The Mongols at some point had to withdraw because the cold temperature caused supply shortages and high horse mortality (Amedroz 1902). At the same time, the besieged inhabitants of the town were dying from lack of food (Makrizi 1845, II: 81-82) and the intense cold, either in the winter of 1258-59 or 1259-60, the timeline is not clear) (Bedrosian 1986).

Increased precipitation through 1258 and 1259 was beneficial to the grass productivity of the Syrian steppes, since normally semiarid conditions temporarily turned to a more temperate climate. Therefore, in the specific case of the invasion of Syria in 1259–60, lower temperatures and higher precipitation during the summer season most likely caused by volcanic forcing favored the 'tsunami' strategy (May 2016), by allowing a greater number of horses than the region would normally support, albeit for a short period. While the region remained unsuitable for feeding hundreds of thousands of horses for a long period of time, under climatic mitigation it supported temporarily a large army. On the downside, such an army severely depleted the land through overgrazing, and a return to hot conditions posed strict limits on the horses (and livestock) that could be supported. This conclusion can be inferred from recent studies that have formalized environmental responses to climatic variability in relations to grasslands and pastoral resources, (Dangal et al. 2017, 2037-40; Alemayehu and Fantahun 2012; Kgosikoma and Batisani 2014; Begszsuren et al. 2004). As mentioned in section 2.4, semi-arid environments show great sensitivity of both temperature and rainfall changes, which affect biomass production, and thus carrying capacity. Pastures can be negatively affected by overgrazing if the number of herbivores to be fed is greater than the carrying capacity, thus further reducing available resources.

Hülegü left his base in the Mughan steppes in September 1259 and began the invasion of Syria by taking a string of cities in the Jazīra region (Tab. 1, 27-28) (Amitai 1987). Some of the areas in this region appeared to be especially verdant in the fall of 1259, a fact that may indicate above average rainfall during the summer of that year (Boyle 1968). After a series of successful operations against the cities of what is today south-eastern Turkey and northeast Syria, the Mongol army crossed the Euphrates in early January 1260, thus repeating the seasonal pattern of the attack against Baghdad to avoid operations possibly lasting into the summer. Although some sources speak of as many as 120,000 soldiers (Jackson 1980), the Mongol army probably included only about 60,000 Mongol soldiers and several thousands of auxiliaries, including Armenian, Georgian, Muslim and Western European warriors, with horses that may be estimated around 300,000 (Amitai-Preiss 1995; SMITH 1984). On January 25, Aleppo fell after a week's siege, and Damascus was taken in February (Fig. 1B). In March or April, the bulk of Hülegü's army returned to Iran, leaving in Syria according to most estimates, between 10,000 and 20,000, but most likely closer to the lower figure (Smith 1998, Jackson 1980; Jackson 2005, 120; Schütz 1991; Thorau, 1985) led by Ketbuqa, Hülegü's most experienced and valued commander (Tab. 1, 30-36).

While Hülegü stated in a letter to Louis IX that he had left Syria because the pastures had been exhausted, it is remarkable that his army could operate for as long as it did in northern Syria (Mevyaert 1980; Richard 2005; Morgan 1985). It is, however, difficult to estimate how many soldiers and horses could have been supported by the available pastures, in the northern Syrian steppes. A recent study (Mawlawi and Tawil 1990), estimates the total number of horses bred in Syria in 1983 at 50,000. While we cannot make a direct comparison with the environmental characteristics of 1260, and while other estimates may be somewhat higher (Amitai-Preiss 1995; Smith 1984), it is likely that the horses left in Syria were the most that the region could support, especially considering that the land had been previously depleted by the impact of the campaign, and that other animals raised by local pastoralists, such as sheep and camels, were using the same resources.

In the spring and summer of 1260 Ketbuqa conducted a series of military operations to suppress local rebellions and consolidate Mongol political and military control (Amitai-Preiss 1995). These operations did not require massive military power and could be easily managed with the forces at hand. Over the summer, however, the Mamluk Sultan Qutuz managed to put together a military force by unifying till-then divided civil and military leaders from Egypt and Syria. This force, probably amounting to 12,000–15,000 Mamluk soldiers, marched northward into Palestine (Jackson 1980; Amitai-Preiss 1995; SMITH 1984), where they received logistical support from the Franks (Crusaders) in Acre. Early skirmishes were fought with a Mongol detachment under Baidar, who withdrew temporarily while Ketbuqa hurriedly gathered the Mongol army scattered around Damascus. He reached the area of ᶜAyn Jālūt, near the Jezreel Valley, possibly because the area was rich in water and grass for the horses (Fig. 1B, star; Fig. 2B; Tab. 1, 37), with a force that comprised around 10,000 soldiers, and possibly tired (Schütz 1991). The armies met in battle on 3 September 1260, when the Mongols were defeated and routed after a day of fierce combat and the death of Ketbuqa himself (Amitai-Preiss 2017, 2021). On the heels of their victory, the Mamluks proceeded to rid Syria of any remaining Mongol presence. Later wars by the Ilkhans (the Mongol dynasty ruling

Iran) to recover Syria also resulted in defeat and the establishment of a militarized frontier between the two powers (Amitai-Preiss 1999). Historians agree that the low number of Mongol troops was a decisive factor in the Mongol debacle and subsequent Mamluk invasion of Syria, even though the betrayal by coerced Syrian 'allies' on the battlefield (Levi della Vida 1935; Amitai-Preiss 1995), and the support offered by the Franks to Qutuz were contributing factors.

The Mongol so-called 'tsunami strategy' (May 2016, 11-37) consisted of bringing into a hostile region an overwhelming number of soldiers to subdue the enemy, to be later withdrawn with the exception of a small force employed to establish control and transition to civilian rule. This strategy was used successfully in the attack against the Caliphate in Baghdad and in the invasion of Syria. However, given the massive logistical requirements, the carrying capacity of the land was the determining factor in planning the scale and timing of the military operations. The success of the strategy was therefore predicated on a meticulous balancing of territorial resources, number of horses, and people mobilized. In a semiarid climate, the timing was dictated by the need to complete operations before the onset of the hot and dry season, lasting from April to November. This is why the major military operations against Baghdad and in Syria were carried out in winter (December–February). The same conditions of cool and wet climate, however, had a different effect in the more mountainous region of northern Iran, the Caucasus and parts of Anatolia, where they prolonged and hampered the siege of Mayyafariqin, and possibly immobilized part of Hülegü's army for about a year (1258–59) (Amitai-Preiss 2011). As a point of comparison to assess the possible effects of short-term climatic downturns in Syria, we may consider that when Timur (Tamerlane) invaded Syria in 1401, his army suffered a loss of 3,000 soldiers caused by cold weather (Raphael 2013, 104). Such a loss was evidently large enough to be regarded as exceptional.

4 Conclusions

While our climatic analysis remains preliminary and not fully substantiated by spatially explicit proxy records, it is sufficiently clear to allow the formulation of a hypothesis that may provide a new understanding of the Mongol defeat at ᶜAyn Jālūt. Climate variability and environmental changes were implicated in the following ways. First, colder conditions may have been a primary factor in slowing down the Mongol armies, and were responsible for some of the difficulties in the military operations of 1258 and 1259. Secondly, and concurrently, increased precipitation during the summers of 1258 and 1259 presumably boosted net primary productivity in the normally semiarid regions of Eastern Anatolia and Syria when the campaign resumed in late 1259, supporting a greater number of animals. The above-average availability of grass and water allowed the Mongol army to field a larger number of horses and soldiers than would have been possible under normal conditions, taking control of the territory and achieving their military objectives in a short time. However, the large number of horses likely caused the rapid depletion of land resources by overgrazing, as reported in the above-mentioned letter by Hülegü to the king of France. Third, the exhaustion of pasturage and of concomitant return to warmer and drier conditions allowed for support of only a limited additional number of soldiers, who proved sufficient to assert control over the region, but not to resist the invasion of the well-trained Mamluk army. Fourth, leaving a limited number of troops carried political consequences, because intelligence about the low number of Mongols was one of the main arguments used by Qutuz to persuade Muslim officers to join his anti-Mongol campaign (Hebraeus 1932). Whether or not the Mongols might have foreseen the Mamluk attack, their defensive capabilities could not have exceeded the force assembled in Syria, which represented their maximum potential in the region, and the ultimate reason for their defeat.

Based on the close examination of the impact of climate variability in the aftermath of the Samalas eruption in ~1257 on the Mongol conquest of the Middle East (1258–60), we conclude that colder and wetter conditions attributable to the largest volcanic eruption in the past 2,500 years extended the reach of the Mongol conquest into Syria, but overgrazing, as well as a return to arid conditions, forced the Mongols to withdraw most of their forces, contributing to their defeat by the Mamluks at ᶜAyn Jālūt. Combining high-resolution climate data from proxy reconstructions and state-of-the-art model simulations with evidence from documentary sources, this study reveals hidden connections between historical and natural events, thus proposing a new interpretation of an important event in world history. Furthermore, without attributing causality to climate variability, we stress the connection between environmental resources and their potential and actual uses as a critical element in decision-making in premodern societies, suggesting a direct linkage to both territorial knowledge and the goals they aimed to achieve.

Acknowledgments

We thank Professor Reuven Amitai (Hebrew University, Jerusalem) for his kind comments. Martino Diez provided helpful assistance. We remain solely responsible for all mistakes. Ulf Büntgen received funding from SustES – Adaptation strategies for sustainable ecosystem services and food security under adverse environmental conditions (CZ.02.1.01/0.0/0.0/16_019/0000797), and the ERC project MONOSTAR (AdG 882727).

References

Abdulahi, M. M.; Hashim, H. and Teha, M. (2016): Rangeland degradation: extent, impacts, and alternative restoration techniques in the rangelands of Ethiopia. In: Tropical and Subtropical Agroecosystems, 19 (3).

Alemayehu, K. and Fantahun, T. (2012): The effect of climate change on ruminant livestock population dynamics in Ethiopia. In: Livestock Research for Rural Development 24.10.

Alizadeh, K. and Ur, J.-A. (2007): Formation and destruction of pastoral irrigation landscapes on the Mughan Steppe, northwestern Iran. In: Antiquity 81.311, 148–160. https://doi.org/10.1017/S0003598X00094904

Amedroz, H. F. (1902): Three Arabic MSS. On the History of the City of Mayyāfāriqīn. In: The Journal of the Royal Asiatic Society of Great Britain and Ireland, 785–812. https://doi.org/10.1017/S0035869X00029816

Amitai, R. (1987): Mongol raids into Palestine (AD 1260 and 1300). In: The Journal of the Royal Asiatic Society of Great Britain and Ireland 2, 236–255. https://doi.org/10.1017/S0035869X0014064X

Amitai-Preiss (1995): Mongols and Mamluks: the Mamluk-Ilkhanid war (1260-1281). Cambridge.

(1999): Northern Syria between the Mongols and Mamluks: Political boundary, military frontier, and ethnic affinities. In: Power, D. and Standen, N. (eds.): Frontiers in question. London, 128–152.

(2011): Im Westen nichts Neues? Re-examing Hülegü Offensive into the Jazīra and Northern Syria in light of recent research. In: Krämer, F.; Schmidt, K.; and Singer, J. (eds.): Historicizing the ‘Beyond’. The Mongolian invasion as a new dimension of violence. Heidelberg, 83–96.

(2017): ᶜAyn Jālūt Revisited. In: France, J. (ed.): Medieval warfare 1000–1300. Oxfordshire, 363–394.

(2021): Back to ᶜAyn Jālūt, again. In: Jerusalem Studies in Arabic and Islam 50, 225–254.

Bedrosian (ed.) (1986): Kirakos Ganjakets’ i’s History of the Armenians. New York.

Begzsuren, S.; Ellis, J. E.; Ojima, D. S.; Coughenour, M. B.; and Chuluun, T. (2004) Livestock responses to droughts and severe winter weather in the Gobi Three Beauty National Park, Mongolia. In: Journal of Arid environments 59.4, 785–796. https://doi.org/10.1016/j.jaridenv.2004.02.001

Boyle, J. A. (1968): Dynastic and political history of the Ilkhans. In: Fisher, W. B.; Boyle, J. A. and Frye, R. N. (eds.): The Cambridge History of Iran. Cambridge, 303–421. https://doi.org/10.1017/CHOL9780521069366.005

(ed.) (1958): The History of the world-conqueror by ‘Alā-ad-Dīn ‘Ata-Malik Juvainī. 2 vols. Manchester.

Büntgen, U. and Di Cosmo, N. (2016): Climatic and environmental aspects of the Mongol withdrawal from Hungary in 1242 CE. In: Scientific Reports 6, 25606. https://doi.org/10.1038/srep25606

Büntgen, U. and Oppenheimer, C. (2020): The importance of ‘year zero’ in interdisciplinary studies of climate and history. In: Proceedings of the National Academy of Science, USA 117, 32845–32847. https://doi.org/10.1073/pnas.2018103117

Büntgen, U.; Arseneault, D.; Boucher, É.; Churakova (Sidorova), O.-V.; Gennaretti, F.; Crivellaro, A.; Hantemirov, R.; Hughes, M.-K.; Kirdyanov, A.; Klippel, L.; Krusic, P.-J.; Linderholm, H.-W.; Ljungqvist, F.-C.; Ludescher, J.; Mccormick, M.; Myglan, V.-S.; Nicolussi, K.; Piermattei, A.; Oppenheimer, C.; Reinig, F.; Sigl, M.; Vaganov, E.-A.; and Esper, J. (2020): Prominent role of volcanism in Common Era climate variability and human history. In: Dendrochronologia 64, 125757. https://doi.org/10.1016/j.dendro.2020.125757

Büntgen, U.; Frank, D.-C.; Nievergelt, D. and Esper, J. (2006): Summer temperature variations in the European Alps, AD 755-2004. In: Journal of Climate 19 (2), 5606–5623. https://doi.org/10.1175/JCLI3917.1

Büntgen, U.; Franke, J.; Frank, D.; Wilson, R.; Gonzales-Rouco, F.; and Esper, J. (2010): Assessing the spatial signature of European climate reconstructions. In: Climate Research 41, 125–130. https://doi.org/10.3354/cr00848

Büntgen, U.; Myglan, V.-S.; Charpentier Ljungvist, F.; Mccormick, M.; Di Cosmo, N.; Sigl, M.; Junclaus, J. et al. (2016): Cooling and societal change during the Late Antique Little Ice Age from 536 to around 660 AD. In: Nature Geoscience 9 (3), 231–236. https://doi.org/10.1038/ngeo2652

Büntgen, U.; Tegel, W.; Nicolussi, K.; Mccormick, M.; Frank, D.; Trouet, V.; Kaplan, J.-O. et al. (2011): 2500 years of European climate variability and human susceptibility. In: Science 331 (6017), 578–582. https://doi.org/10.1126/science.1197175

Büntgen, U.; Krusic, P.- J.; Verstege, A.; Sangüesa-Barreda, G.; Wagner, S.; Camarero, J.-J.; Charpentier Ljungqvist, F. et al. (2017): New tree-ring evidence from the Pyrenees reveals Western Mediterranean climate variability since medieval times. In: Journal of Climate 30 (14), 5295–5318. https://doi.org/10.1175/JCLI-D-16-0526.1

Cook, E.-R.; Seager, R.; Kushnir, Y.; Briffa, K.-R.; Büntgen, U.; Frank, D.; Krusic, P.J. et al. (2015): Old World megadroughts and pluvials during the Common Era. In: Science Advances 1 (10), 1500561. https://doi.org/10.1126/sciadv.1500561

Crowley, T.-J. and Unterman, M.-B. (2013): Technical details concerning development of a 1200 yr proxy index for global volcanism. In: Earth System Science Data 5 (1), 187. https://doi.org/10.5194/essd-5-187-2013

Dangal, S. R.; Tian, H.; Lu, C.; Ren, W.; Pan, S.; Yang, J.; Di Cosmo, N. and Hessl, A. (2017): Integrating herbivore population dynamics into a global land biosphere model: plugging animals into the earth system. In: Journal of Advances in Modeling Earth Systems 9 (8), 2920–2945. https://doi.org/10.1002/2016MS000904

Dashdondog, B. (2010): The Mongols and the Armenians (1220-1335). Leiden.

Di Cosmo, N.; Hessl, A.; Leland, C.; Byambasuren, O.; Tian, H.; Nachin, B.; Pederson, N.; Andreu-Hayles, L. and Cook, E. R. (2018): Environmental stress and steppe nomads: rethinking the history of the Uyghur Empire (744–840) with paleoclimate data. In: Journal of Interdisciplinary History 48 (4), 439–463. https://doi.org/10.1162/JINH_a_01194

Di Cosmo, N.; Oppenheimer, C. and Büntgen, U. (2017): Interplay of environmental and socio-political factors in the downfall of the Eastern Türk Empire in 630 CE. In: Climatic change, 145 (3-4), 383–395. https://doi.org/10.1007/s10584-017-2111-0

Esper, J.; Frank, D.; Bütgen, U., Verstege, A.; Luterbacher, J. and Xoplaki, E. (2007): Long-term drought severity variations in Morocco. In: Geophysical Research Letters 34 (17). https://doi.org/10.1029/2007GL030844

Esper, J.; Konter, O.; Klippel, L.; Reinig, F.; Krusic, P.-J. and Büntgen, U. (2021): Pre-instrumental summer precipitation variability in northwestern Greece from a high-elevation Pinus heldreichii network. In: International Journal of Climatology. https://doi.org/10.1002/joc.6992

Ganiev, R. T. and Kukarskih, V. V. (2019): Natural disasters in the history of the Eastern Turk Empire. In: Liang, E. Y.; Bork, H.-R.; Fang, X. and Mischke, S. (eds.): Socio-environmental dynamics along the historical silk road. Cham, 177–193. https://doi.org/10.1007/978-3-030-00728-7

Gao, C.; Robock, A. and Ammann, C. (2008): Volcanic forcing of climate over the past 1500 years: an improved ice core-based index for climate models. In: Journal of Geophysical Research: Atmospheres 113 (D23). https://doi.org/10.1029/2008JD010239

Garibaldi, L. A.; Semmartin, M. and Chaneton, E .J. (2007): Grazing-induced changes in plant composition affect litter quality and nutrient cycling in flooding Pampa grasslands. In: Oecologia 151, 650–662. https://doi.org/10.1007/s00442-006-0615-9

Giorgetta, M.-A.; Jungclaus, J.-H.; Reick, C.-H.; Legutke, S.; Bader, J.; Böttinger, M.; Brovkin, V. et al. (2013): Climate and carbon cycle changes from 1850 to 2100 in MPI-ESM simulations for the Coupled Model Intercomparison Project phase 5. In: Journal of Advances in Modeling Earth Systems 5 (3), 572–597. https://doi.org/10.1002/jame.20038

Griggs, C.; Degaetano, A.; Kuniholm, P. and Newton, M.-A. (2007): Regional high-frequency reconstruction of May–June precipitation in the north Aegean from oak tree rings, AD 1089–1989. In: International Journal of Climatology 27, 1075–1089. https://doi.org/10.1002/joc.1459

Guillet, S.; Corona, C.; Stoffel, M.; Khodri, M.; Lavigne, F.; Ortega, P.; Eckert, N. et al. (2017): Climate response to the Samalas volcanic eruption in 1257 revealed by proxy records. In: Nature Geoscience 10 (2), 123–128. https://doi.org/10.1038/ngeo2875

Han, D.; Wang, G.; Xue, B.; Liu, T.; Yinglan, A. and Xu, X. (2018): Evaluation of semiarid grassland degradation in North China from multiple perspectives. In: Ecological Engineering 112, 41–50. https://doi.org/10.1016/j.ecoleng.2017.12.011

Hebraeus, B. (1932) (edited and translated by Budge, E. A. W.): The chronography of Gregory Abû'l Faraj, the son of Aaron, the Hebrew physician, commonly known as Bar Hebraeus. London.

Jackson, P. (1980): The crisis in the Holy Land in 1260. In: The English Historical Review 95, 481–513. https://doi.org/10.1093/ehr/XCV.CCCLXXVI.481

(2005): The Mongols and the West: 1221-1410. London.

(2017): The Mongols and the Islamic world: from conquest to conversion. New Haven.

Jungclaus, J.-H.; Lohmann, K. and Zanchettin, D. (2014): Enhanced 20th century heat transfer to the Arctic simulated in context of climate variations over last millennium. In: Climate of the Past 10, 2201–2213. https://doi.org/10.5194/cp-10-2201-2014

Kgosikoma, O. E. and Batisani, N. (2014): Livestock population dynamics and pastoral communities' adaptation to rainfall variability in communal lands of Kgalagadi South, Botswana. In: Pastoralism 4, 1-9. https://doi.org/10.1186/s13570-014-0019-0

Klippel, L.; Krusic, P.-J.; Brandes, R.; Hartl, C.; Belmecheri, S.; Dienst, M. and Esper, J.-A. (2018): 1286-year hydro-climate reconstruction for the Balkan Peninsula. In: Boreas 47, 1218–1229. https://doi.org/10.1111/bor.12320

Landrum, L.; Otto-Bliesner, B.-L.; Wahl, E.-R.; Conley, A.; Lawrence, P.-J.; Rosenbloom, N. and Teng, H. (2013): Last millennium climate and its variability in CCSM4. In: Journal of Climate 26 (4), 1085–1111. https://doi.org/10.1175/JCLI-D-11-00326.1

Lane, G. (1999): Arghun Aqa: Mongol bureaucrat. In: Iranian Studies 32 (4), 459–482. https://doi.org/10.1080/00210869908701965

Le Houérou, H. N.; Bingham, R. L. and Skerbek, W. (1988): Relationship between the variability of primary production and the variability of annual precipitation in world arid lands. In: Journal of Arid Environments 15 (1), 1–18. https://doi.org/10.1016/S0140-1963(18)31001-2

Levi della Vida, G.-L. (1935): L'invasione dei Tartari in Siria nel 1260 nei ricordi di un testimone oculare. In: Orientalia 4, 353–376.

Louhaichi, M. and Tastad, A. (2010): The Syrian steppe: past trends, current status, and future priorities. In: Rangelands 32 (2), 2–7. https://doi.org/10.2111/1551-501X-32.2.2

Louhaichi, M.; Ghassali, F.; Salkini, A. K. and Petersen, S. L. (2012): Effect of sheep grazing on rangeland plant communities: case study of landscape depressions within Syrian arid steppes. In: Journal of Arid Environments 79, 101–106. https://doi.org/10.1016/j.jaridenv.2011.11.024

Luterbacher, J.; Newfield, T. P.; Xoplaki, E. et al. (2020): Past pandemics and climate variability across the Mediterranean. In: Euro-Mediterranean Journal for Environmental Integration 5, 46. https://doi.org/10.1007/s41207-020-00197-5

Makrizi,A. (1845): Histoire des sultans mamlouks de l'Égypte. Translated by E. Quatremère. Paris.

Martin, H. D. (1950): The rise of Chingis Khan and His Conquest of North China. Baltimore.

Martínez-Valderrama, J.; Ibáñez, J.; Del Barrio, G.; Alcalá, F. J.; Sanjuán, M. E.; Ruiz, A. and Puigdefábregas, J. (2018): Doomed to collapse: why Algerian steppe rangelands are overgrazed and some lessons to help land-use transitions. In: Science of the Total Environment 613, 1489-1497. https://doi.org/10.1016/j.scitotenv.2017.07.058

Mawlawi, B. and Tawil, M.-W. (1990): The role of legumes in the farming systems of Syria. In: Osman, E.; Ibrahim, M. H. and Jones, M. A. (eds.): The role of legumes in the farming systems of the Mediterranean areas. New York, 105–114. https://doi.org/10.1007/978-94-009-1019-5_10

May, T. (2016): Mongol conquest strategy in the Middle East. In: De Nicola, B. and Melville, C. (eds.): The Mongols' Middle East: continuity and transformation in Ilkhanid Iran. Leiden, 11–37. https://doi.org/10.1163/9789004314726_003

Meyvaert, P. (1980): An unknown letter of Hulagu, Il-Khan of Persia, to king Louis IX of France. In: Viator 11, 245–260. https://doi.org/10.1484/J.VIATOR.2.301508

Morgan, D. (1985): The Mongols in Syria, 1260-1300. In: Edbury, P.–W. and Smail, R.-C. (eds.): Crusade and Settlement. Cardiff, 231-235.

Oppenheimer, C.; Wacker, L.; Xu J.; Galván, J. D.; Stoffel, M.; Guillet, S.; Corona, C. et al (2017): Multi-proxy dating the 'Millennium Eruption' of Changbaishan to late 946 CE. In: Quaternary Science Reviews 158, 164-171. https://doi.org/10.1016/j.quascirev.2016.12.024

Pederson, N.; Hessl, A.; Baatarbileg, N.; Anchukaitis, K.-J. and Di Cosmo, N. (2014): Pluvials, droughts, the Mongol Empire, and modern Mongolia. In: Proceedings of the National Academy of Science, USA 111, 12, 4375–4379. https://doi.org/10.1073/pnas.1318677111

Piermattei, A.; Crivellaro, A.; Krusic, P. J.; Esper, J.; Vítek, P.; Oppenheimer, C.; Felhofer, M.; Gierlinger, N.; Reinig, F.; Urban, O.; Verstege, A.; Lobo, H. and Büntgen, U. (2020): A millennium-long 'Blue-Ring' chronology from the Spanish Pyrenees reveals sever ephemeral summer cooling after volcanic eruptions. In: Environmental Research Letters 15, 124016. https://doi.org/10.1088/1748-9326/abc120

Pongratz, J.; Reick, C.; Raddatz, T. and Claussen, M. (2008): A reconstruction of global agricultural areas and land cover for the last millennium. In: Global Biogeochemical Cycles 22 (3). https://doi.org/10.1029/2007GB003153

Potts, D.-T. (2014): The Mongols and Timurids. In: Potts, D.-T. (ed.): Nomadism in Iran: from antiquity to the modern era. Oxford, 189–213. https://doi.org/10.1093/acprof:oso/9780199330799.003.0006

Putnam, A. E.; Putnam, D. E.; Andreu-Hayles, L.; Cook, E. R.; Palmer, J. G.; Clark, E. H. and Broecker, W. S. (2016): Little Ice Age wetting of interior Asian deserts and the rise of the Mongol Empire. In: Quaternary Science Reviews 131, 33–50. https://doi.org/10.1016/j.quascirev.2015.10.033

Qi, S.; Zheng, H.; Lin, Q.; Li, G.; Xi, Z. and Zhao, X. (2011): Effects of livestock grazing intensity on soil biota in a semiarid steppe of Inner Mongolia. In: Plant and Soil 340 (1), 117–126. https://doi.org/10.1007/s11104-010-0463-6

Raphael, S. K. (2013): Climate and political climate. Leiden. https://doi.org/10.1163/9789004244733

Richard, J. (2005): La lettre de Hülegü à Saint Louis et l'entente avec les Mongols. In: Richard, J. (ed.) : Au-delà de la Perse et de l'Arménie: l'Orient latin et la découverte de l'Asie intérieure: quelques textes inégalement connus aux origines de l'alliance entre Francs et Mongols (1145-1262). Brepols, 175–193. https://doi.org/10.1484/M.MMA-EB.4.00230

Schütz, E. (1991): The decisive motives of Tatar failure in the Ilkhanid - Mamluk fights in the Holy Land. In: Acta Orientalia Academiae Scientiarum Hungaricae 45 (1), 3–22.

Sigl, M.; Winstrup, M.; Mcconnell, J.-R.; Welten, K.-C.; Plunkett, G.; Ludlow, F.; Bütgen, U. et al. (2015): Timing and climate forcing of volcanic eruptions for the past 2,500 years. In: Nature 523 (7562), 543–549. https://doi.org/10.1038/nature14565

Smith Jr., J.-M. (1984): ^{c}Ayn Jālūt: Mamluk success or Mongol failure? In: Harvard Journal of Asiatic Studies, 307–345. https://doi.org/10.2307/2719035

(1998): Nomads on ponies vs. slaves on horses. In: Journal of the American Oriental Society 118. 1, 54–62. https://doi.org/10.2307/606298

(2006): Hülegü moves west: high living and heartbreak on the road to Baghdad. In: Komaroff, L. (ed.): Beyond the legacy of Genghis Khan. Leiden, 111–134.

Stoffel, M.; Khodri, M.; Corona, C.; Guillet, S.; Poulain, V.; Bekki, S.; Guiot, J. et al. (2015): Estimates of volcanic-induced cooling in the Northern Hemisphere over the past 1,500 years. In: Nature Geoscience 8 (10), 784–788. https://doi.org/10.1038/ngeo2526.

Sullivan, S. and Rohde, R. (2002): Guest editorial: On non-equilibrium in arid and semi-arid grazing systems. In: Journal of Biogeography 29 (12), 1595–1618. https://doi.org/10.1046/j.1365-2699.2002.00799.x

Thackston, W. (ed.) (2012): Classical writings of the medieval Islamic world. Persian histories of the Mongol conquest. Vol. 3: Jami'u't-Tawarikh: In: Compendium of Chronicles by Rashiduddin Fazlullah, 341–44. https://doi.org/10.5040/9780755607235

Thorau, P. (1985): The battle of ^{c}Ayn Jālūt: A Re-examination. In: Edbury, P.–W. and Smail, R.-C. (eds.): Crusade and settlement. Cardiff, 236–41.

Uppala, S. M. et al. (2005): The ERA-40 Re-Analysis. In: The Quarterly Journal of the Royal Meteorological Society 131 (612), 2961–3012. https://doi.org/10.1256/qj.04.176

Vidal, C. M.; Métrich, N.; Komorowski, J.-C.; Pratomo, I.; Michel, A.; Kartadinata, N.; Robert, V. and Lavigne, F. (2016): The 1257 Samalas eruption (Lombok, Indonesia): the single greatest stratospheric gas release of the Common Era. In: Scientific Reports 6, 34868. https://doi.org/10.1038/srep34868

Vieira, L.-E.-A.; Solanki, S.-K.; Krivova, N.-A. and Usoskin, I. (2011): Evolution of the solar irradiance during the Holocene. In: Astronomy & Astrophysics 531, A6. https://doi.org/10.1051/0004-6361/201015843

Wade, D. C.; Vidal, C. M.; Abraham, N. L.; Dhomse, S.; Griffiths, P. T.; Keeble, J.; Mann, G.; Marshall, L.; Schmidt, A. and Archibal, A. T. (2020): Reconciling the climate and ozone response to the 1257 CE Mount Samalas eruption. In: Proceedings of the National Academy of Science, USA. https://doi.org/10.1073/pnas.1919807117

Wiesmeier, M.; Kreyling, O.; Steffens, M.; Schoenbach, P.; Wan, H.; Gierus, M. and Kögel-Knabner, I. (2012): Short-term degradation of semiarid grasslands - results from a controlled-grazing experiment in Northern China. In: Journal of Plant Nutrition and Soil Science 175 (3), 434–442. https://doi.org/10.1002/jpln.201100327

Xie, Y. and Sha, Z. (2012): Quantitative analysis of driving factors of grassland degradation: a case study in Xilin River Basin, Inner Mongolia. In: The Scientific World Journal 2012. https://doi.org/10.1100/2012/169724

Zhao, H. L.; Zhao, X. Y.; Zhou, R. L.; Zhang, T. H. and Drake, S. (2005): Desertification processes due to heavy grazing in sandy rangeland, Inner Mongolia. In: Journal of arid environments 62 (2), 309–319. https://doi.org/10.1100/2012/169724

Authors

Prof. Dr. Nicola Di Cosmo
Institute for Advanced Study
School of Historical Studies
08540 Princeton
NJ
USA
ndc@ias.edu

Dr. Sebastian Wagner
Helmholtz-Zentrum Hereon
Institute of Coastal Systems
21502 Geesthacht
Germany

Prof. Dr. Ulf Büntgen
Department of Geography
University of Cambridge
Cambridge CB2 3EN
UK
ulf.buentgen@geog.cam.ac.uk

Simulated temperature and precipitation anomalies from winter 1256–57 to summer 1260 based on the MPI-ESM-P_r1 model

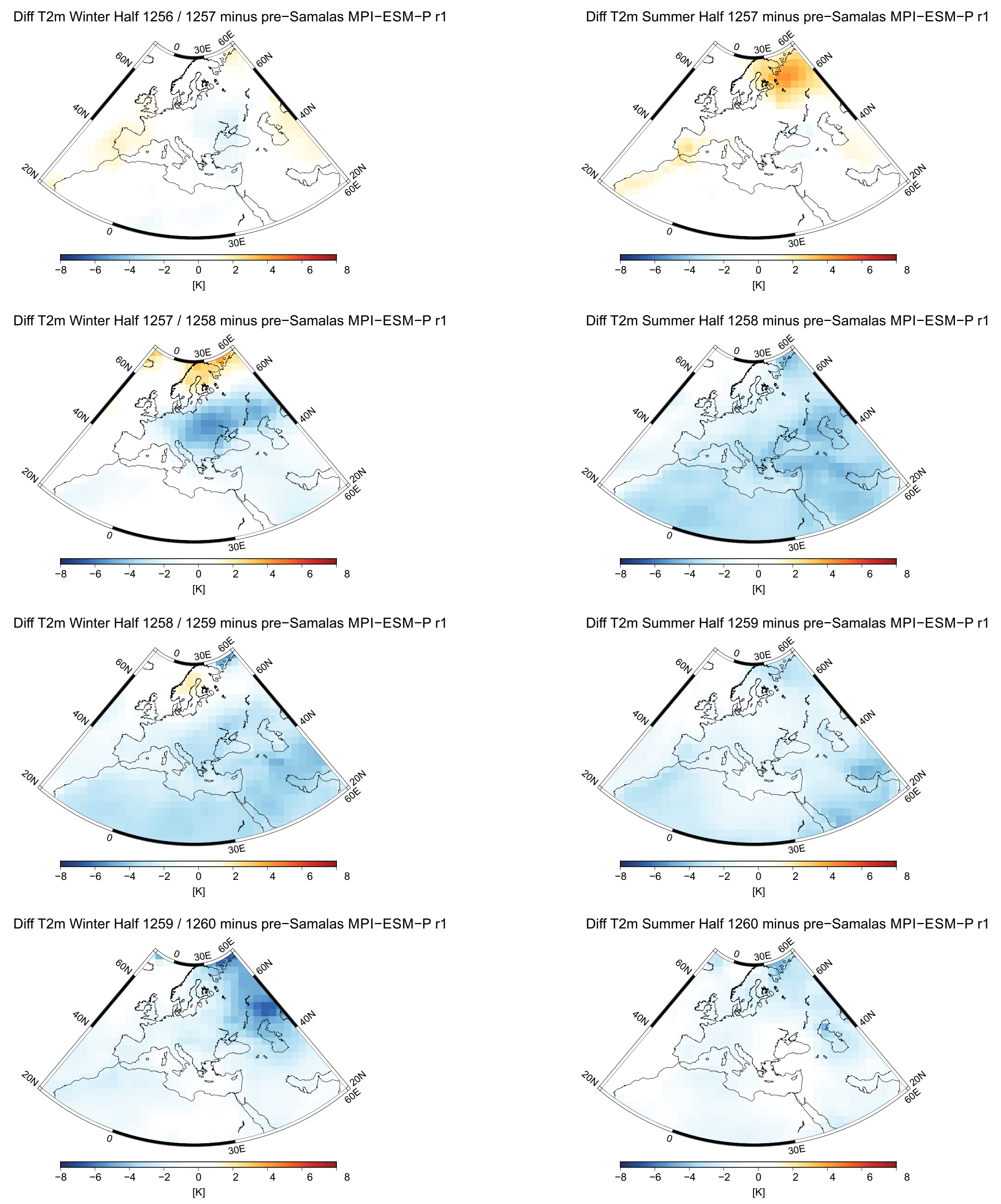

Fig. S1: Simulated temperature anomalies from winter 1256–57 to summer 1260. Based on the MPI-ESM-P_r1 model, maps on the left and right sides refer to the six-month average winter (October–March) and summer (April–September) summer seasons, respectively. All values are in Kelvin, and expressed as anomalies to the pre-Samalas period 1225–1254.

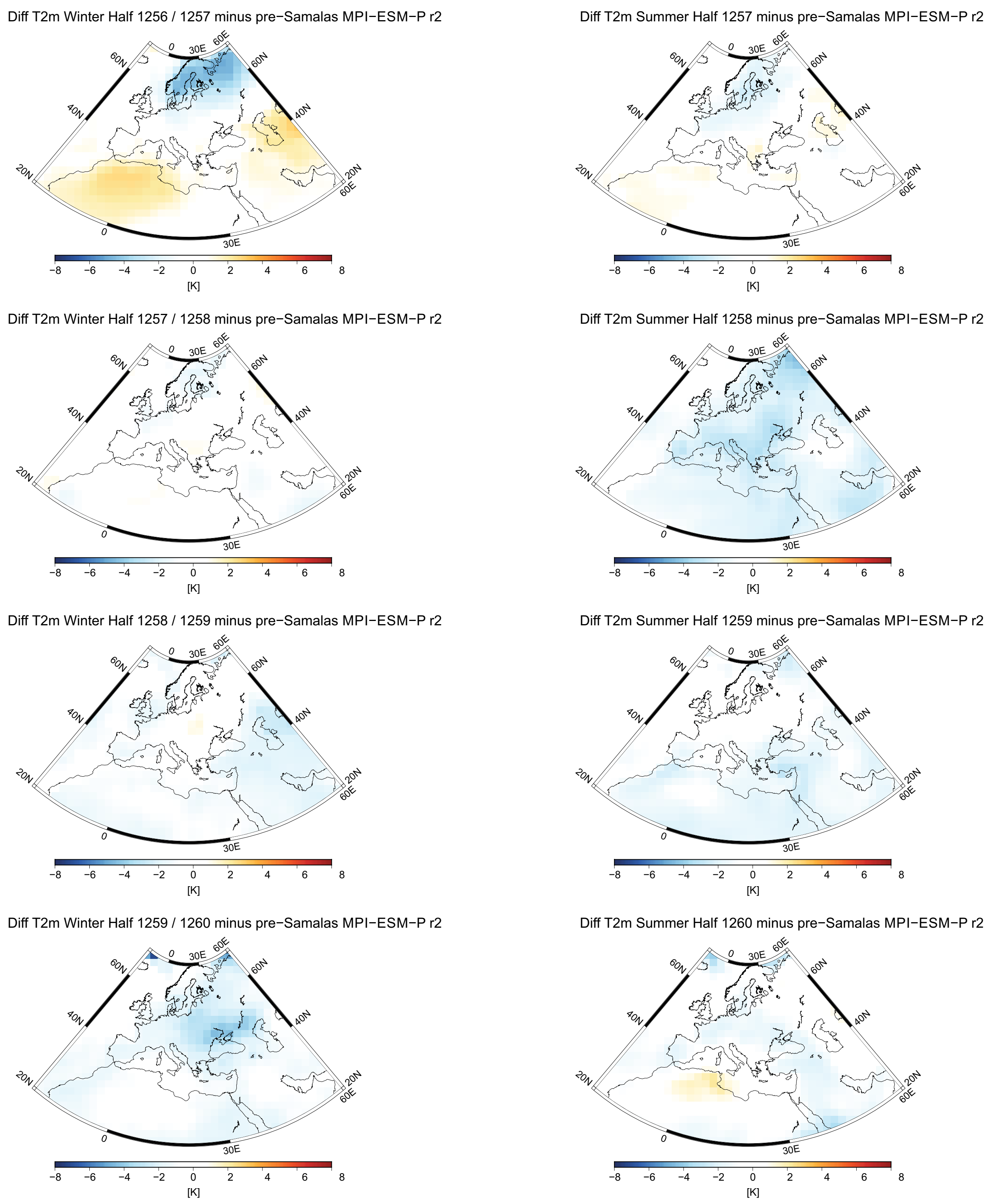

Fig. S2: Simulated temperature anomalies from winter 1256–57 to summer 1260. Based on the MPI-ESM-P_r2 model, maps on the left and right sides refer to the six-month average winter (October–March) and summer (April–September) summer seasons, respectively. All values are in Kelvin, and expressed as anomalies to the pre-Samalas period 1225–1254.

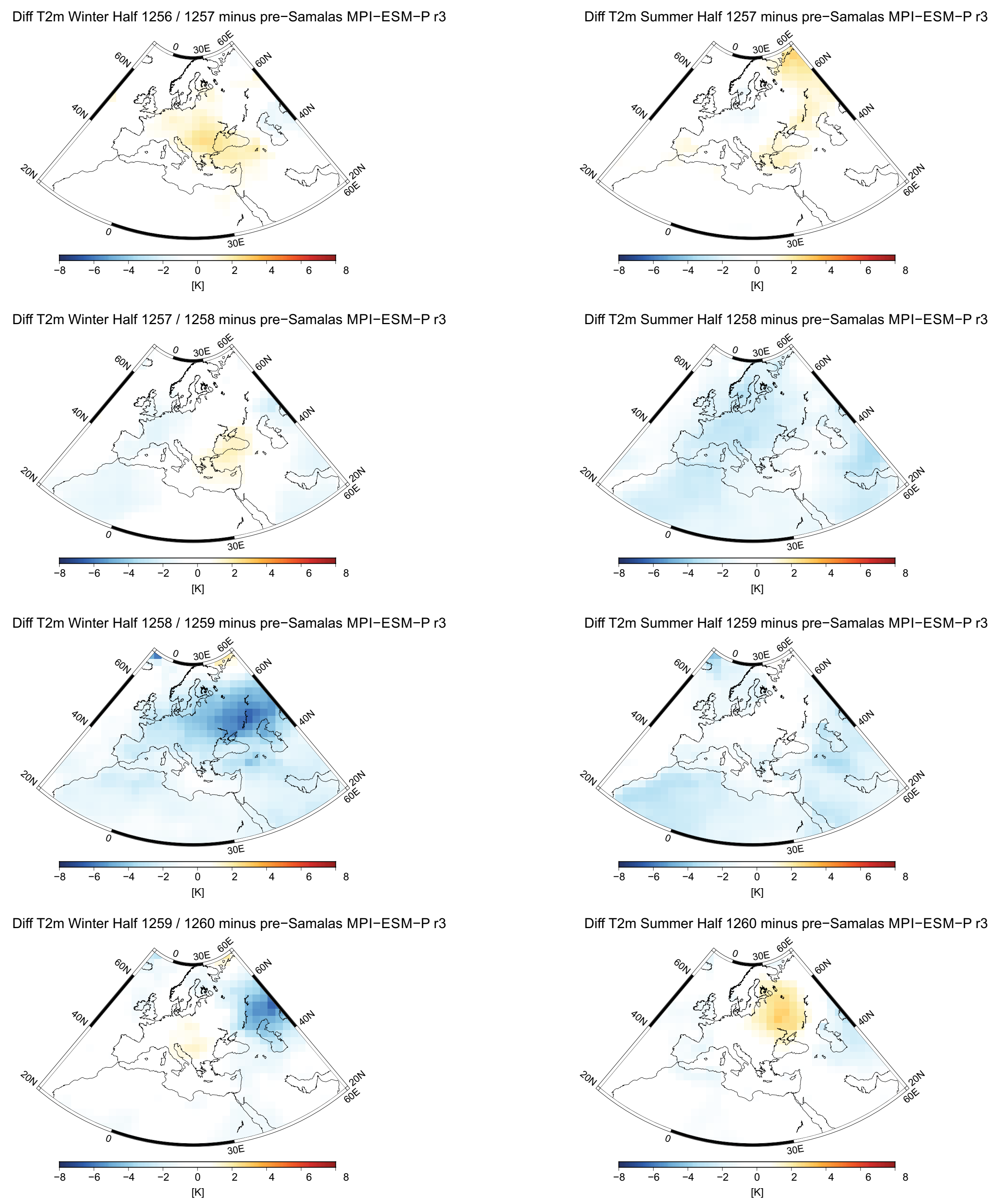

Fig. S3: Simulated temperature anomalies from winter 1256–57 to summer 1260. Based on the MPI-ESM-P_r3 model, maps on the left and right sides refer to the six-month average winter (October–March) and summer (April–September) summer seasons, respectively. All values are in Kelvin, and expressed as anomalies to the pre-Samalas period 1225–1254.

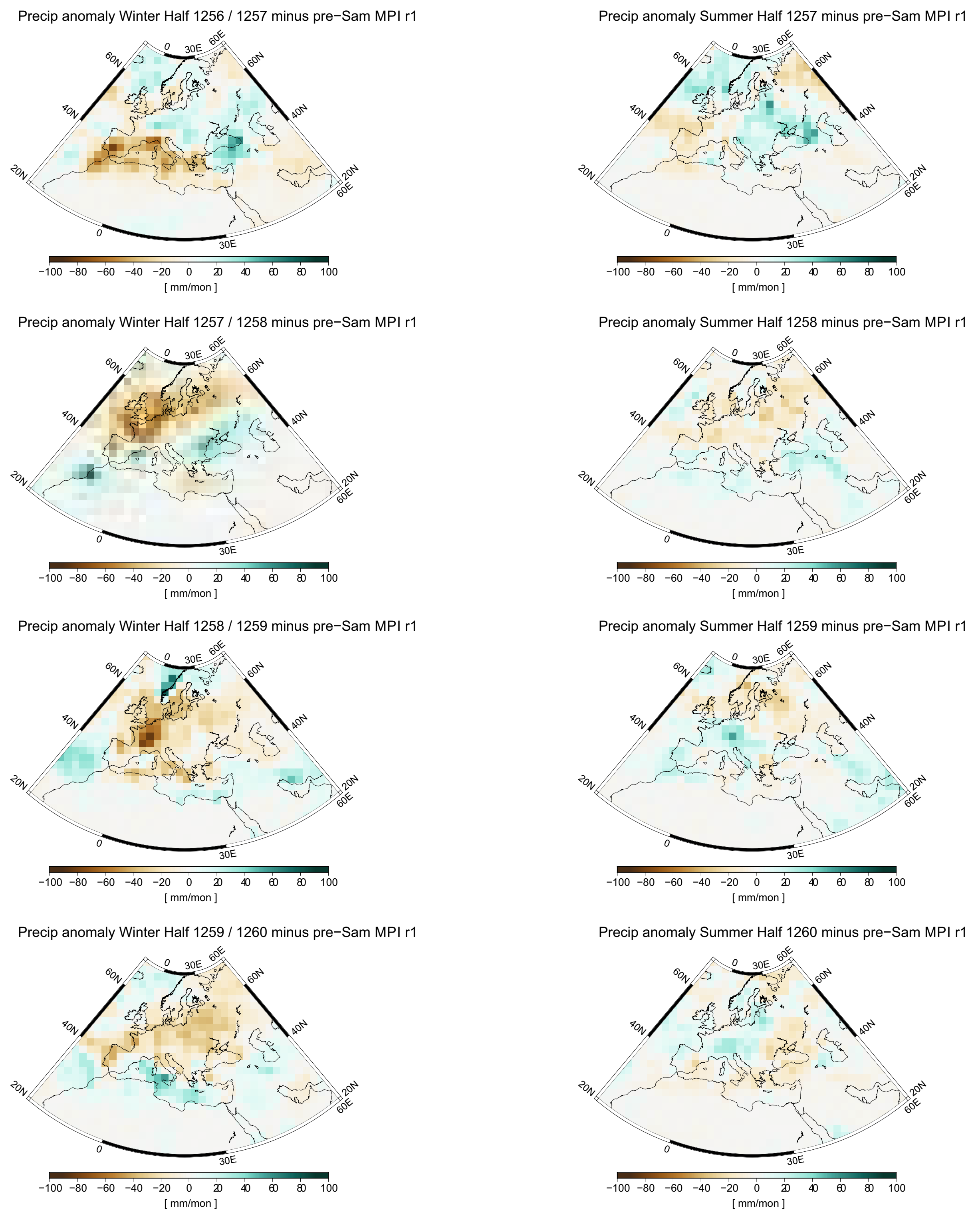

Fig. S4: Simulated precipitation anomalies from winter 1256–57 to summer 1260. Based on the MPI-ESM-P_r1 model, maps on the left and right sides refer to the six-month average winter (October–March) and summer (April–September) summer seasons, respectively. All values are in millimeter per month, and expressed as anomalies to the pre-Samalas period 1225–1254.

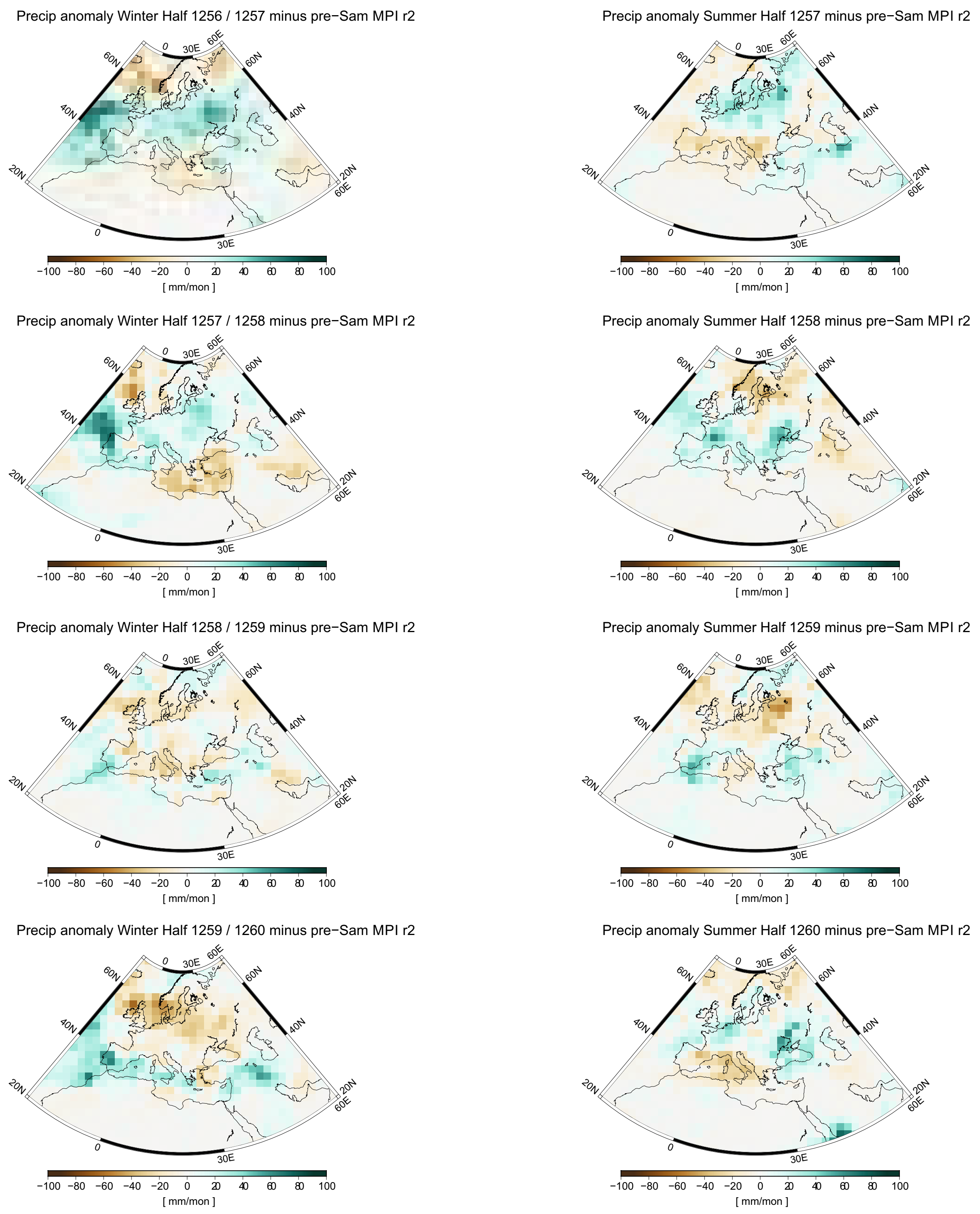

Fig. S5: Simulated precipitation anomalies from winter 1256–57 to summer 1260. Based on the MPI-ESM-P_r2 model, maps on the left and right sides refer to the six-month average winter (October–March) and summer (April–September) summer seasons, respectively. All values are in millimeter per month, and expressed as anomalies to the pre-Samalas period 1225–1254.

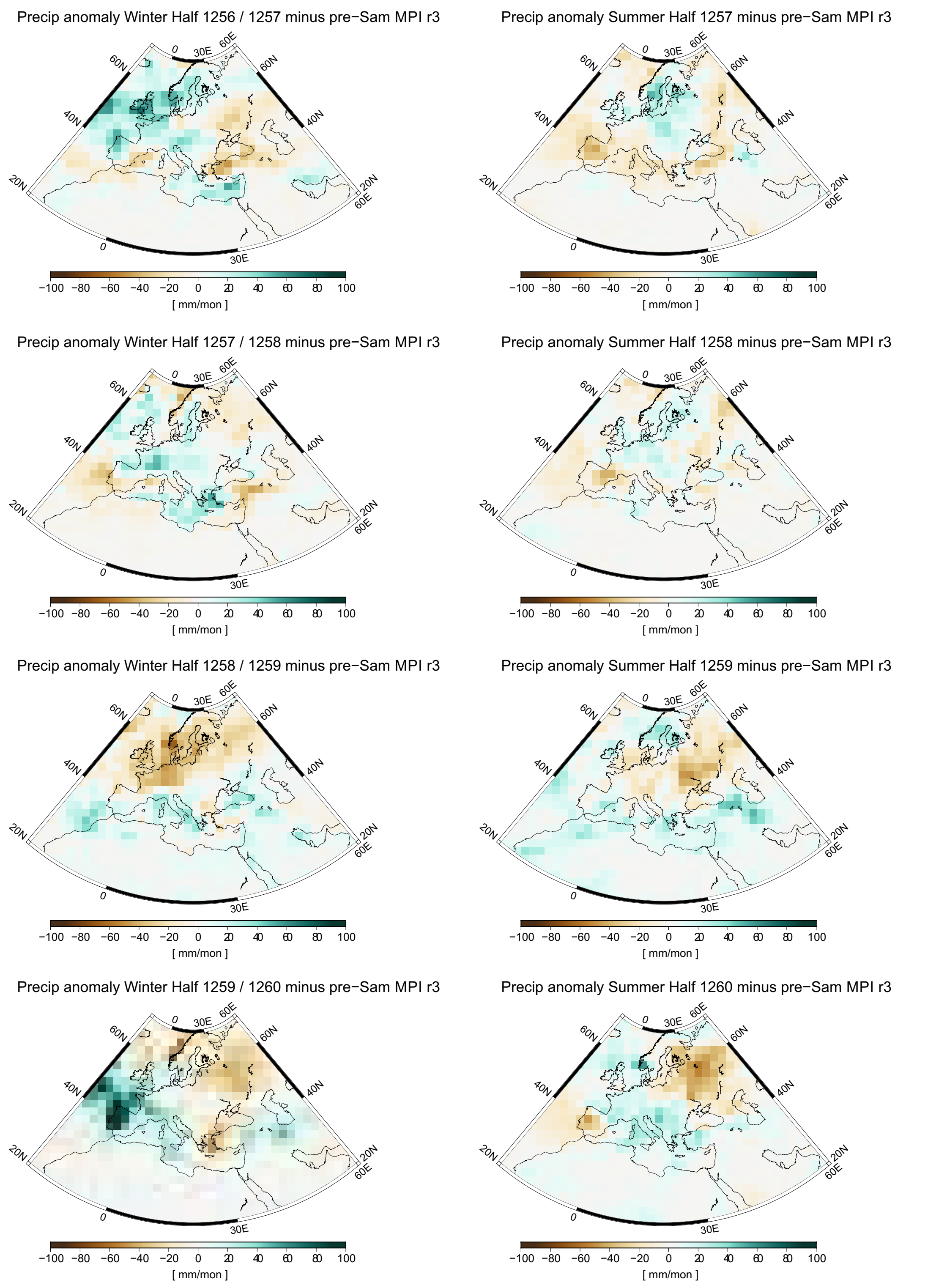

Fig. S6: Simulated precipitation anomalies from winter 1256–57 to summer 1260. Based on the MPI-ESM-P_r3 model, maps on the left and right sides refer to the six-month average winter (October–March) and summer (April–September) summer seasons, respectively. All values are in millimeter per month, and expressed as anomalies to the pre-Samalas period 1225–1254.